INFLUENCE OF Ni ADDITION ON MICROSTRUCTURE AND SOLIDIFICATION BEHAVIOUR OF SAC305 LEAD-FREE SOLDERS

UDC:621.791.3
Original scientific paper https://doi.org/10.46793/aeletters.2025.10.2.4

Tereza Machajdíková[1*], Roman Čička[1], Ivona Černičková[1], Libor Ďuriška[1], Marián Drienovský[1], Peter Gogola[1], Jakub Perička[2]

[1]Slovak University of Technology in Bratislava, Faculty of Materials Science and Technology in Trnava, Institute of Materials, Trnava, Slovakia
[2]Slovak University of Technology in Bratislava, Faculty of Materials Science and Technology in Trnava, Institute of Applied Informatics, Automation and Mechatronics, Trnava, Slovakia

Abstract:
This study investigates the addition of Ni into SAC305 solder alloy with varying nickel content (0–4 wt.% Ni) using experimental techniques and computational thermodynamics. The experimental part employed various techniques (scanning electron microscopy, X-ray diffraction, energy-dispersive X-ray spectroscopy, and differential scanning calorimetry). The microstructure of the investigated alloys consisted of primary β-Sn and an eutectic mixture containing β-Sn and two intermetallic compound particles (Ag_3Sn and Cu_6Sn_5). Small Ni additions (up to 0.2 wt.%) refined the microstructure and significantly reduced the undercooling from 30°C (SAC305) to about 12°C. However, Ni additions exceeding 0.4 wt.% led to microstructural coarsening and formation of Ni_3Sn_4 phase. For the computational part, Thermo-Calc software was used to investigate the conditions of Cu_6Sn_5 and Ni_3Sn_4 phase formation. The experimental results were consistent with computations from Thermo-Calc. The results suggest that minor Ni additions (up to 0.2 wt.%) offer possibilities to refine the microstructure and reduce undercooling, potentially improving the properties of solders.

ARTICLE HISTORY
Received: 16 April 2025
Revised: 6 June 2025
Accepted: 17 June 2025
Published: 30 June 2025

KEYWORDS
SAC305, Nickel addition, Phase composition, Undercooling, Computational thermodynamics

1. INTRODUCTION

In the past, practically all microelectronic assemblies used eutectic Sn-Pb solders, with the most popular being 63Sn-37Pb and 60Sn-40Pb. These solders have been used in the electronics industry for over 50 years, mostly due to their superior soldering properties, manufacturability, reliability, and low price. However, lead can cause harm to the environment and is toxic to humans. Exposure to lead is inevitable during the soldering process, as people can be exposed through lead-containing dust from solder dross. Lead can also enter groundwater when old electronic products are discarded in landfills and subsequently harm ecosystems and wildlife [1,2]. Due to these issues, Sn-Pb solders were eliminated from electronic devices by the Environmental Protection Agency (EPA) [3]. This restriction has been the main driving force for the development of lead-free solders. As the world moves towards more sustainable and environmentally friendly manufacturing practices, the role of lead-free solders becomes increasingly important in electronics production. Solder alloys play a crucial role in the electronic industry as they serve as electrical and mechanical connections to other components in electronic devices [4,5]. In the past decades, there has been an intense search for a suitable replacement for the traditional Sn-Pb solder alloys. Among the various lead-free solders, Sn-Ag-Cu (SAC) alloys have been accepted as the most promising replacement, mainly due to their

*CONTACT: Tereza Machajdíková, e-mail: tereza.machajdikova@stuba.sk

suitable combination of properties, such as good solderability, reliability, and excellent creep resistance [6-9]. According to the European Lead-free Technology Roadmap [10], near-eutectic SAC alloys with 3-4 wt.% Ag and 0.5-1 wt.% Cu are the most widely accepted solders due to their excellent wettability, high creep resistance, and relatively low melting temperature compared to the Sn-Ag binary eutectic alloy. The addition of Cu improves wettability and lowers the melting temperature. One disadvantage of SAC solders is that their melting point is higher than that of Sn-Pb solders. Other disadvantages include higher cost (primarily due to the inclusion of silver), the need for careful flux selection to avoid oxidation during re-flow soldering [10], the formation of large and brittle intermetallic compounds (IMCs), high undercooling, and the formation of undesired Cu_3Sn phase at the SAC/Cu interface [11]. Despite these disadvantages, SAC alloys are widely used in many electronic devices [10].

The key trend in the development of lead-free solders is the investigation of the influence of other elements on the properties of SAC solders. Elements such as Zn, Al, In, Ni, Bi, Ga, rare-earth elements, and even nanoparticles have been utilized to modify the Sn-based lead-free solders [8,11-16]. Ni has attracted considerable interest as an alloying addition due to its ability to enhance the properties of the SAC solder alloy [17-23]. Hammad [24] found that small additions of Ni (0.05 – 0.1 wt.%) led to microstructural refinement, as the microstructure is composed of small rod-shaped $(Cu,Ni)_6Sn_5$ IMCs in β-Sn matrix. Due to this microstructure, the SAC-Ni solder shows higher tensile strength. Hammad and El-Taher [25] and Che et al. [26] found that minor additions of Ni (0.02 and 0.05 wt.%) have the potential to improve the shear strength of SAC solder. According to El-Daly et al. [27], the addition of 0.5 wt.% of Ni led to lower undercooling and improvement in the creep resistance of the alloy. From the research done by Nogita [28]; and Nogita and Nishimura [29], the addition of 0.05 wt.% of Ni leads to the stabilization of Cu_6Sn_5 in high-temperature hexagonal form. Yang et al. [30] investigated different additions of Ni (0.05, 0.5 and 1 wt.%) into SAC305 and found that it can lead to the suppression of the Cu_3Sn growth at the solder/Cu interface. Similar effects on intermetallic layers at the solder/Cu interface were also found when Ni nanoparticles (0.2 – 1.0 wt.%) were added to Sn-58Bi solder alloy [31].

In the development of new lead-free solders, computational thermodynamics is often used as a tool for predicting and optimizing alloy compositions and properties. Using computational methods, such as the CALPHAD approach, it is possible to simulate the relationships between material properties, phase stability, and phase composition in multi-component solder systems. This allows for the prediction of many important properties, including melting temperature, phase equilibria, intermetallic phase formation, and microstructural evolution.

In this work, the different additions of Ni on microstructure and solidification behaviour of SAC lead-free solder are investigated using different experimental techniques such as scanning electron microscopy (SEM), energy-dispersive spectroscopy (EDX), X-ray diffraction (XRD), and differential scanning calorimetry (DSC). Experimental conclusions are then compared to calculations in Thermo-Calc. The findings about the influence of Ni on the microstructure, formation and stability of Cu_6Sn_5 and Ni_3Sn_4 phases and solidification behaviour of SAC305 solder are presented. Computational thermodynamics was used to explain the occurrence of phases and the compositions obtained experimentally, to understand the influence of Ni.

2. MATERIALS AND METHODS

Sn-3.0Ag-0.5Cu (SAC305) alloys with different additions of Ni (0 - 4 wt.%), as given in Table 1, were investigated using experimental techniques and computational thermodynamics. The eight alloys were prepared from raw materials Sn, Ag, Cu, and Ni (of 99,99% purity). They were mixed in proper fractions, and the overall mass of the mixtures was 50 grams. Then the mixtures were melted in an induction furnace under an argon atmosphere. For the microstructural analysis, metallographic preparation was carried out by standard procedures consisting of grinding (60#, 240#, 600#, 1200#, and 4000# SiC paper), polishing by diamond suspension (9, 6, 3, and 1 μm) and finally ultrasonic polishing. The microstructures of the solder alloys were analyzed by scanning electron microscopy using JEOL JSM-7600F in backscattered electrons mode. The distribution of elements was analyzed by the energy dispersive X-ray spectroscopy using Oxford Instruments X-max 50. X-ray diffraction analysis was used to identify the phases present in the system. This analysis was carried out on powder samples, where XRD patterns were recorded in 2Theta mode in the range (20÷120)° using a PANalytical Empyrean instrument with a PIXCel3D detector at

40kV and 40mA. Cu-Kα radiation was used with a step size of 0.026° and a counting time of 96 seconds per pixel per step. For the evaluation of XRD patterns HighScore software was used with the following ICSD cards 98-010-6071 (β-Sn), 98-000-2721 (Ag_3Sn), 98-010-6530 (Cu_6Sn_5), 98-010-5363 (Ni_3Sn_4). Quantitative analysis of X-ray diffraction patterns was performed using the Rietveld refinement program MAUD (version 2.9995). Experimental peaks were fitted using an asymmetric pseudo-Voigt function. Instrumental broadening was accounted for by analyzing the NIST660c LaB6 standard (National Institute of Standards and Technology, Gaithersburg, MD, USA) for line position and broadening, and these parameters were incorporated into the Rietveld refinement via the Caglioti equation. The weighted profile R-factor (R_{wp}) for all analyzed samples was below 10%, indicating a reliable quality of fit. To analyze the melting and solidification behaviour of the samples, differential scanning calorimetry was carried out using Pyris Diamond DSC (PerkinElmer). The calibration of DSC was performed using In, Sn, Pb, and Zn standards. All of the measurements were done under a nitrogen (purity 5.0) protective atmosphere. All of the samples used for the analysis were cut from the bulk specimens with a mass of about 5.5 mg and were sealed in an aluminum pan. The samples were flat-shaped to ensure good thermal contact with aluminum pan bottom. Five measuring cycles in the temperature range (30-250)°C for each sample were carried out, with a heating rate of 10°/min and a cooling rate of 20°C/min. Finally, computational thermodynamics was used to explain the formation of Cu_6Sn_5 and Ni_3Sn_4 phases. Thermo-Calc software (version 2023b) and the thermodynamic database of lead-free solder systems (TCSLD, version 4.1) were used for all calculations.

Table 1. Compositions of the investigated samples (in wt.%)

No.	Alloy	Ag	Cu	Ni	Sn
1	SAC305	3.0	0.5	-	bal.
2	SAC305-0.05Ni	3.0	0.5	0.05	bal.
3	SAC305-0.1Ni	3.0	0.5	0.1	bal.
4	SAC305-0.15Ni	3.0	0.5	0.15	bal.
5	SAC305-0.2Ni	3.0	0.5	0.2	bal.
6	SAC305-0.4Ni	3.0	0.5	0.4	bal.
7	SAC305-1Ni	3.0	0.5	1	bal.
8	SAC305-4Ni	3.0	0.5	4	bal.

3. RESULTS

3.1 Microstructural Analysis

Ten different places in the central part were selected for each sample for qualitative analysis of microstructure. The as-cast microstructures of some SAC305-xNi (x=0, 0.1, 0.4, and 4 wt.%) are shown in Fig. 1. The SAC305 alloy shows a microstructure consisting of primary β-Sn grains surrounded by eutectic mixture containing β-Sn and two IMC particles (Ag_3Sn and Cu_6Sn_5). With the addition of Ni, the microstructure of SAC305 changes; a small addition of Ni (0.05, 0.1, 0.15, and 0.2 wt.%) leads to refinement of the eutectic microstructure. A very fine eutectic microstructure was found in SAC305-0.05Ni sample, with the amount of Ni, the eutectic microstructure starts to be slightly coarsened. From 0.4 wt% addition of Ni, the Cu_6Sn_5 phase becomes significantly coarser and with a higher addition of Ni (1 and 4 wt.%) Ni_3Sn_4 phase starts to form, with very coarse morphology. From the EDX analysis performed on the solder alloys (Fig.2a and Fig.2b), it was found that Ni diffuses into Cu_6Sn_5, forming a (Cu,Ni)6Sn5 phase, but only till 1 wt.% Ni addition. At higher amount of Ni most of the Ni forms the Ni_3Sn_4 phase. It was implied by Cheng et al. [22] that the Ni atom could accelerate the formation of $(Cu,Ni)_6Sn_5$ phase and replace some fraction of Cu in the $(Cu,Ni)_6Sn_5$ phase, thus stabilizing this phase.

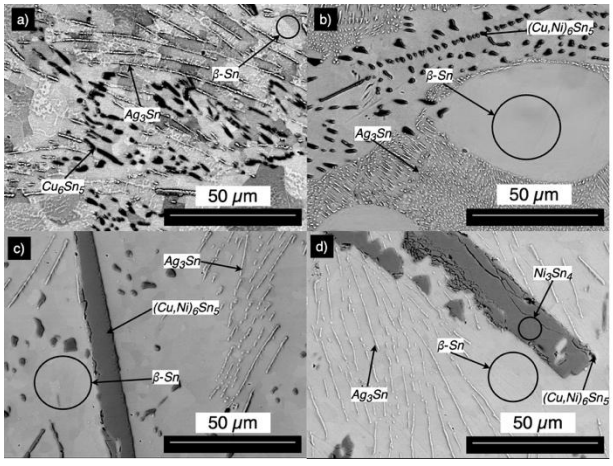

Fig. 1. As-cast microstructures of SAC305 (a), SAC305-0.1Ni (b), SAC305-0.4Ni (c), SAC305-4Ni (d), using SEM

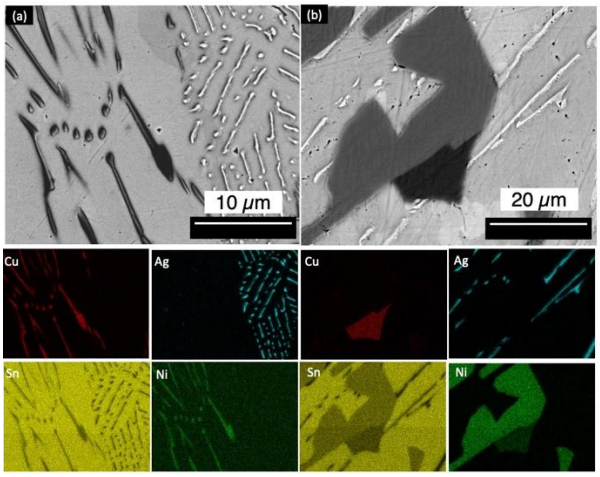

Fig. 2. As-cast microstructures and elemental distributions (Cu, Ag, Sn, Ni) using SEM+EDX; SAC305-0.1Ni (a), SAC305-4Ni (b)

The presence of all phases was further verified by XRD analysis, using two measuring runs for each sample to check repeatability. Typical measured diffraction patterns are shown in Fig.3. The results confirmed the presence of β-Sn, Ag_3Sn, a small amount of Cu_6Sn_5 in most samples, and Ni_3Sn_4 phase in samples containing 1 and 4 wt.% Ni. The amount of each phase was quantified using Rietveld refinement and predicted in Thermo-Calc, the graph showing these results is in Fig.4. Overall, good agreement was achieved between SEM+EDX, XRD experiments, and phase compositions calculated in Thermo-Calc. Both experimental (EDX maps) and computational results (Thermo-Calc) confirmed only negligible solubility of Ni in β-Sn and Ag_3Sn phases.

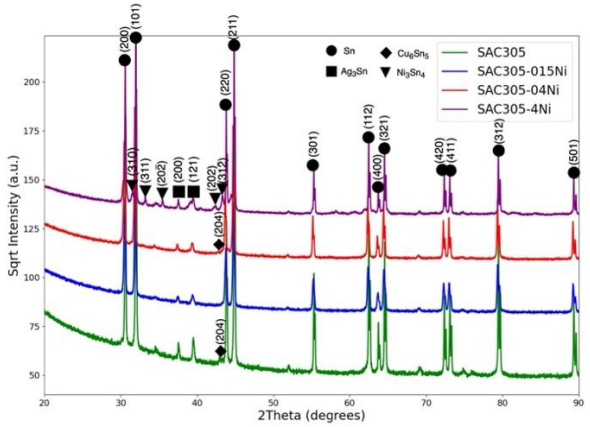

Fig. 3. X-ray diffraction of SAC305-xNi (x=0,0.15,0.4, and 4 wt.%)

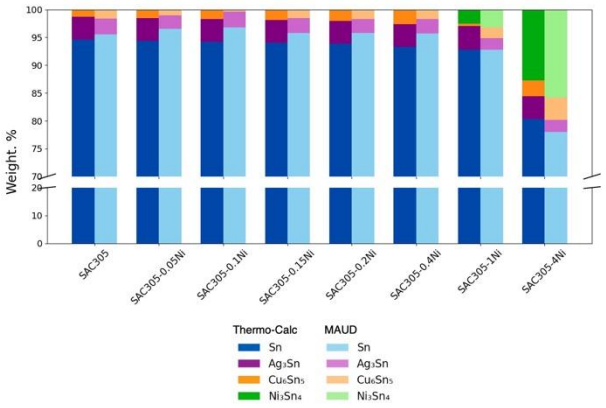

Fig. 4. Comparison of phase amounts of SAC305-xNi predicted in Thermo-Calc (left columns) and experimentally obtained by XRD (right columns)

3.2 Thermal Analysis (DSC)

Five runs were performed for each sample during DSC measurements. The DSC profiles for SAC305-xNi (x=0, 0.15, 0.2, and 4 wt.%) are shown in Fig.5. It shows both the endothermic and exothermic peaks, corresponding to melting and solidification processes upon heating and cooling of the samples. It can be seen that relatively high undercooling occurs in the case of sample SAC305 (Fig.5a). In case of samples SAC305-015Ni and SAC305-02Ni two thermal events are clearly visible at lower undercoolings (Fig.5b and Fig.5c). In case of sample SAC305-4Ni again the increased undercooling was observed (Fig.5d). The eutectic temperatures during heating and cooling of all the samples are given in Table 2 (average values and standard deviations from 5 measurement runs) and illustrated in Fig.6, red and blue circles denote the average temperatures. On the left side of the figure, it can be seen that the eutectic temperature slightly rises (from 219 to 221)°C with the addition of Ni. On the right side of the figure, the difference in eutectic temperature during heating and cooling is shown, illustrating the undercooling of samples. For the solder joints, a lower undercooling is desirable. The undercooling decreases with the addition of Ni, but only till SAC305-0.2Ni, at higher amounts of Ni it starts to increase. It was observed, however, that the addition of Ni, even at the higher amount, decreased the undercooling in comparison to the original SAC305. This suggests that the minor addition of Ni is effective in reducing the undercooling of the SAC305 solder.

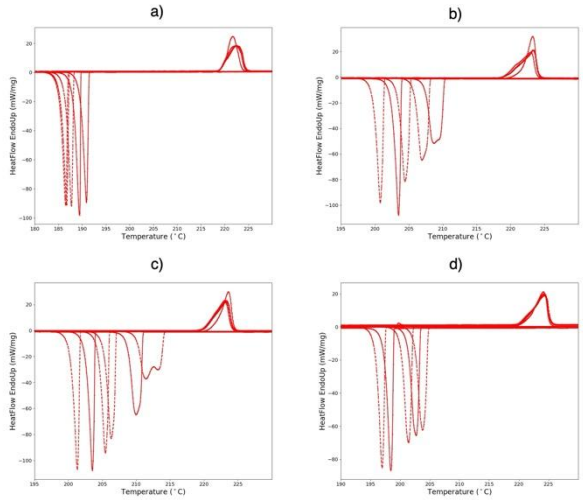

Fig. 5. DSC curves of SAC305 (a), SAC305-0.15Ni (b), SAC305-0.2Ni (c), SAC305-4Ni, (d) during heating and cooling

Table 2. Eutectic temperatures (T_E) of SAC305-xNi samples during heating and cooling

Sample	T_E during heating		T_E during cooling	
	Value (°C)	Standard deviation (°C)	Value (°C)	Standard deviation (°C)
SAC305	218.96	0.055	188.72	1.886
SAC305-0.05Ni	218.80	0.158	195.14	1.305
SAC305-0.1Ni	218.98	0.239	201.98	2.003
SAC305-0.15Ni	219.38	0.370	205.80	3.491
SAC305-0.2Ni	220.10	0.235	208.42	4.072
SAC305-0.4Ni	220.40	0.122	207.88	2.039
SAC305-1Ni	221.04	0.089	206.34	0.643
SAC305-4Ni	220.12	0.192	201.38	3.085

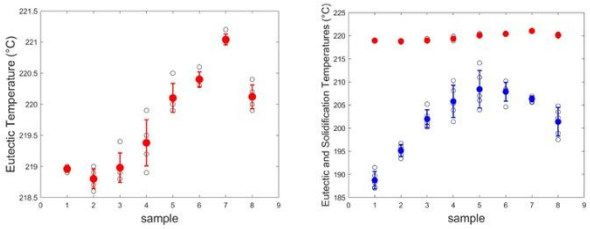

Fig. 6. Eutectic temperatures of SAC305-xNi samples during heating (left) and comparison of temperatures of eutectic transformation during heating and cooling (right), illustrating the undercooling of samples; red circles – heating, blue circles – cooling (average values)

3.3 Thermodynamic Computations

The experimental results demonstrate that the addition of Ni to the SAC305 solder alloy significantly affects microstructure, particularly regarding $(Cu,Ni)_6Sn_5$ and Ni_3Sn_4 phases. Fig. 7, derived from Thermo-Calc calculations, illustrates these effects for various Ni concentrations. At lower Ni additions (0.05, 0.1, 0.15, 0.2, and 0.4 wt.%), Ni was observed to dissolve entirely within the $(Cu,Ni)_6Sn_5$ phase, enhancing its formation. This trend is reflected in the increasing molar fraction of the $(Cu,Ni)_6Sn_5$ phase with increasing Ni content up to 0.4 wt.%. At higher Ni concentrations (1 and 4 wt.%), a new phase of Ni_3Sn_4 begins to form, with only a minor portion of Ni continuing to dissolve in $(Cu,Ni)_6Sn_5$. At 1 wt.% Ni, a minor amount of Ni_3Sn_4 is formed. However, at 4 wt.% Ni, the amount of $(Cu,Ni)_6Sn_5$ drastically reduces to approximately 1 mol.%, while the Ni_3Sn_4 phase increases significantly, reaching about 20 mol.%. These findings explain the behaviour of Ni in phase formations during solidification. It means that at lower amounts of Ni (up to 0.4 wt.%) Ni is incorporated in $(Cu,Ni)_6Sn_5$ phase (substituing Cu), increasing the amount of $(Cu,Ni)_6Sn_5$. At higher amounts of Ni (from 0.4 wt.%), Ni is incorporated in the newly formed Ni_3Sn_4 phase.

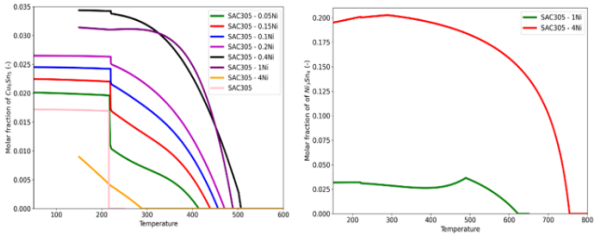

Fig. 7. Molar fractions of Cu_6Sn_5 (left) and Ni_3Sn_4 (right) in dependence on temperature, for SAC305-xNi alloys

4. DISCUSSION

In this work, the phase composition, microstructure and thermal behaviour of SAC305-xNi (x = 0 – 4 wt.%) solders were analyzed. The basic microstructure of samples consisted of β-Sn and eutectics (β-Sn + Ag_3Sn, β-Sn + $(Cu,Ni)_6Sn_5$). It was observed that the microstructure becomes refined with just a small amount of Ni (0.05 wt.%). With increasing addition of Ni (from 0.1 wt.%) the slight coarsening of microstructure and increasing amount of $(Cu,Ni)_6Sn_5$ (up to 0.4 wt.% Ni) were observed. With further increasing Ni addition (1 wt.%) the phase Ni_3Sn_4 (with coarse morphology) starts to form and due to diffusion of Ni the phase $(Cu,Ni)_6Sn_5$ forms often in the vicinity of Ni_3Sn_4 phase. Increasing addition of Ni (up to 4 wt.%) causes a further increase in the amount of Ni_3Sn_4 and a decrease in the amount of $(Cu,Ni)_6Sn_5$ phase.

DSC analysis has shown that the eutectic temperature of SAC305 is 219°C, with an increasing amount of Ni, it slightly increases to 221°C. The undercooling during solidification decreases from

30°C (sample SAC305) to about 12°C (sample SAC305-02Ni). In the paper of El-Daly et al. [27], the undercooling of SAC305 was determined as 24.2°C, and when adding 0.5 wt.% Ni it decreased to 15.7°C, when adding 1 wt.% Ni the undercooling slightly rises to 16.3°C. Our results thus confirm and refine these findings on how Ni influences the undercooling.

The computational predictions are in good agreement with experimental results in this work, meaning that the approach combining the experimental results and results from computational thermodynamics seems to be very useful in enhancing the knowledge and explaining the phase compositions of the investigated solders. This is the reason why two other issues related to SAC-Ni systems given in [13,21,28-30,32] are now mentioned, and predictions from Thermo-Calc are given.

What is the minimum addition of Ni when Ni_3Sn_4 phase starts to form in SAC105, SAC205 and SAC305 solder alloys?

Some authors describe that in SAC105-xNi solders Ni_3Sn_4 phase already occurred if 0.06 mass% Ni was used [13, 21], while in SAC305-xNi solder Ni_3Sn_4 phase was not mentioned even if 1 mass% Ni was used [27,33]. Using computational thermodynamics, the prediction can be made, and the result is given in Fig.8, where the calculated influence of Ni addition on molar fractions of Ni_3Sn_4 and $(Cu,Ni)_6Sn_5$ phases for SAC305-xNi system at 150°C is shown. It can be seen that from 0.45 mass% Ni the Ni_3Sn_4 should be present in system at this temperature. The same result is also valid for SAC105-xNi system, as the solubility of Ag in Ni_3Sn_4 and $(Cu,Ni)_6Sn_5$ phases is negligible.

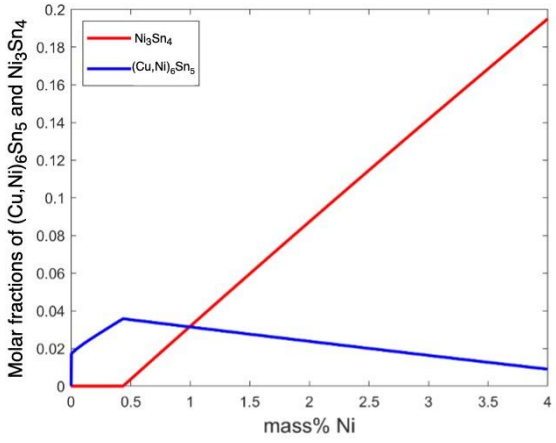

Fig. 8. Molar fractions of Ni_3Sn_4 and $(Cu,Ni)_6Sn_5$ phases in SAC305-xNi system at 150°C in dependence on Ni amount, calculated in Thermo-Calc

What is the minimum amount of Ni addition to stabilize the Cu_6Sn_5 phase in high-temperature hexagonal form in SAC305-xNi system?

Cu_6Sn_5 phase undergoes the phase transformation from high-temperature hexagonal form Cu_6Sn_5(HT) to low-temperature monoclinic phase Cu_6Sn_5(LT) during cooling at 186°C [28,29] with volume change 2.15 vol.%, which could be detrimental for the properties of solders and solder joints. The results of our thermodynamic computations are shown in Fig.9, where the influence of Ni amount on the molar fractions of $(Cu,Ni)_6Sn_5$(HT) and $(Cu,Ni)_6Sn_5$(LT) in SAC305-xNi system at room temperature is shown, together with content of Ni in $(Cu,Ni)_6Sn_5$(HT) phase.

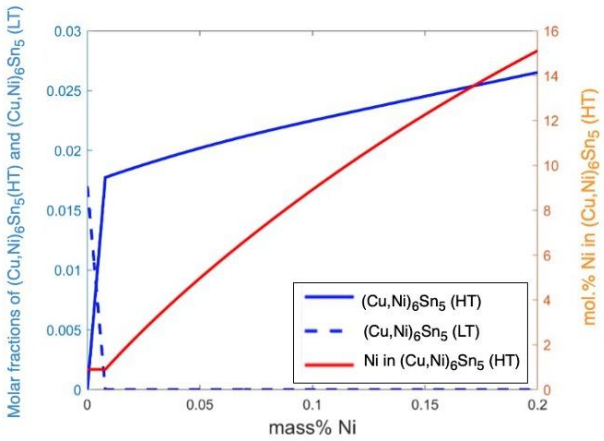

Fig. 9. Molar fractions of $(Cu,Ni)_6Sn_5$(HT) and $(Cu,Ni)_6Sn_5$(LT) phases in SAC305-xNi system at room temperature in dependence on Ni amount (blue curves, left axis) and content of Ni in $(Cu,Ni)_6Sn_5$(HT) phase in dependence on Ni amount (red curve, right axis); calculated in Thermo-Calc

Fig. 10 shows the isopleths Sn-Cu (up to 2 wt.% Cu) of SAC305 alloy and SAC305-0.01Ni. Comparing these isopleths, it can be seen that 0.01 wt.% Ni addition should be sufficient to partially stabilize $(Cu,Ni)_6Sn_5$(HT) phase at room temperature, although from 1.1 wt.% Cu the mixture of $(Cu,Ni)_6Sn_5$(HT) and $(Cu,Ni)_6Sn_5$(LT) is present.

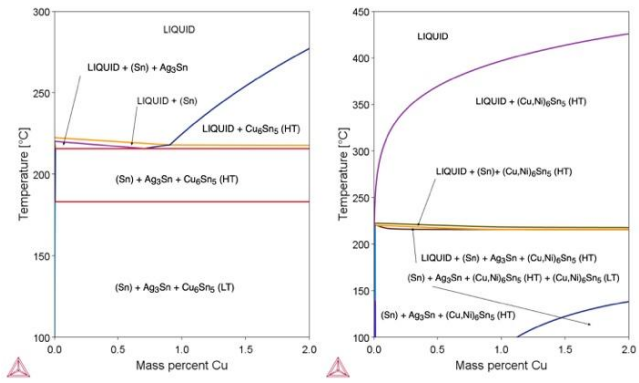

Fig. 10. Isopleths Sn-Cu (up to 2 wt.% Cu) of SAC305 alloy (left) and SAC305-0.01Ni (right), calculated in Thermo-Calc

The effect of Ni on the stabilization of high-temperature (hexagonal) $(Cu,Ni)_6Sn_5$ phase was experimentally investigated by Nogita et al. [28,29,32]. They found that $(Cu,Ni)_6Sn_5$, containing 5 mol.% was stabilized in high-temperature form at low temperatures. Similarly, $(Cu,Ni)_6Sn_5$, containing 9 mol.% was stabilized in high-temperature form at low temperatures. After adding low amounts of phosphorus, the amount of Ni in $(Cu,Ni)_6Sn_5$ decreased to 2 mol.% and the high-temperature $(Cu,Ni)_6Sn_5$ phase transformed to low temperature (monoclinic) phase during cooling. This result could seem to be in contradiction with the computed diagram in Fig.9, where 2 mol.% of Ni should be sufficient to fully stabilize the high-temperature form of $(Cu,Ni)_6Sn_5$. However, our calculations didn't take into account the addition and influence of phosphorus, so strictly speaking, these two cases cannot be compared. The minimum amount of Ni to stabilize $(Cu,Ni)_6Sn_5$ in high-temperature form hasn't been experimentally determined yet.

5. CONCLUSION

The effect of Ni on SAC305 microstructure and undercooling was analysed in this work and several conclusions can be drawn from the experimental results and Thermo-Calc calculations. It was found that minor Ni addition (up to 0.2 wt.%) to SAC305 led to microstructural refinement, with a microstructure consisting of primary β-Sn surrounded by an eutectic mixture containing β-Sn and two intermetallic compound particles (Ag_3Sn and Cu_6Sn_5). The minor addition of Ni (up to 0.4 wt.%) also caused Ni to substitute Cu in the Cu_6Sn_5, leading to the formation of $(Cu,Ni)_6Sn_5$ phase. At 1 wt.% Ni in the microstructure became significantly coarse, with the presence of Ni_3Sn_4 phase, potentially leading to reduced mechanical properties (not analysed in this work) of the solder alloy. The formation of $(Cu,Ni)_6Sn_5$ and Ni_3Sn_4 was also supported by thermodynamic calculations, which showed a good agreement with experiments. The minor additions of Ni (up to 0.4 wt.%) also decreased the undercooling of the SAC305 from 30°C to about 12°C, which can influence the overall properties of the solder alloys.

From these findings it can be concluded that the minor additions (up to 0.2 wt.%) of Ni have a positive effect on the SAC305 solder (refining microstructure, reducing undercooling) and should be studied in more detail, whilst the higher addition (from 0.4 wt.%) of Ni causes coarsening of microstructure and forming of Ni_3Sn_4 phase, generally reducing the properties of solders.

ACKNOWLEDGEMENT

This work was supported by Slovak Research and Development Agency (project APVV-20-0124), the Slovak Grant Agency VEGA (project 1/0389/22), and Young Researcher Grant at MTF STU (project 1343)

CONFLICT OF INTEREST

The authors declare no conflict of interest.

REFERENCES

[1] M.K. Jha, A. Kumari, P.K. Choubey, J.-C. Lee, V. Kumar, J. Jeong, Leaching of lead from solder material of waste printed circuit boards (PCBs). *Hydrometallurgy*, 121-124, 2012: 28-34. https://doi.org/10.1016/j.hydromet.2012.04.010

[2] M. Abtew, G. Selvaduray, Lead-free solders in microelectronics. *Materials Science and Engineering: R: Reports*, 27(5-6), 2000: 95-141 https://doi.org/10.1016/S0927-796X(00)00010-3

[3] S. Menon, E. George, M. Osterman, M. Pecht, High lead solder (over 85%) solder in the electronics industry: RoHS exemptions and alternatives. *Journal of Materials Science: Materials in Electronics*, 26, 2015: 4021-4030. https://doi.org/10.1007/s10854-015-2940-4

[4] N. Jiang, L. Zhang, Z.-Q. Liu, L. Sun, W.-M. Long, P. He, M. Xiong, M. Zhao, Reliability issues of lead-free solder joints in electronic devices. *Science and Technology of Advanced Materials*, 20(1), 2019: 876-901. https://doi.org/10.1080/14686996.2019.1640072

[5] C.M.L. Wu, D.Q. Yu, C.M.T. Law, L. Wang, Properties of lead-free solder alloys with rare

earth element additions. *Materials Science and Engineering*, 44(1), 2004: 1-44. https://doi.org/10.1016/j.mser.2004.01.001

[6] H.R. Kotadia, P.D. Howes, S.H. Mannan, A review: On the development of low melting temperature Pb-free solders. *Microelectronics Reliability*, 54(6-7), 2014: 1253-1273. https://doi.org/10.1016/j.microrel.2014.02.025

[7] Y. Chi-Yang, Yu, J. Lee, W.-L. Chen, J.-G. Duh, Enhancement of the impact toughness in SnAgCu/Cu solder joints via modifying the microstructure of solder alloy. *Materials Letters*, 119, 2014: 20-23. https://doi.org/10.1016/j.matlet.2013.12.088

[8] Y. Wang, G. Wang, K. Song, K. Zhang, Effect of Ni addition on the wettability and microstructure of Sn2.5Ag0.7Cu0.1RE solder alloy. *Materials & Design*, 119, 2017: 219-224. https://doi.org/10.1016/j.matdes.2017.01.046

[9] S. Wang, Y. Yao, W. Wang, Microstructure and size effect of interfacial intermetallic on fracture toughness of Sn3.0Ag0.5Cu solder interconnects. *Engineering Fracture Mechanics*, 202, 2018: 259-274. https://doi.org/10.1016/j.engfracmech.2018.09.031

[10] I.E. Anderson, B.A. Cook, J.L. Harringa, R.L. Terpstra, Sn-Ag-Cu solders and solder joints: Alloy development, microstructure, and properties. *JOM,* 54, 2002: 26–29. https://doi.org/10.1007/BF02701845

[11] T. Zhu, Q. Zhang, H. Bai, L. Zhao, J. Yan, Investigations on deformation and fracture behaviors of the multi-alloyed SnAgCu solder and solder joint by in-situ observation. *Microelectronics Reliability*, 135, 2022: 114574. https://doi.org/10.1016/j.microrel.2022.114574

[12] T. Zhu, Q. Zhang, H. Bai, L. Zhao, J. Yan, Improving tensile strength of SnAgCu/Cu solder joint through multi-elements alloying. *Materials Today Communications,* 29, 2021: 102768. https://doi.org/10.1016/j.mtcomm.2021.102768

[13] F. Cheng, H. Nishikawa, T. Takemoto. Microstructural and mechanical properties of Sn-Ag-Cu lead-free solders with minor addition of Ni and/or Co. *Journal of Materials Science*, 43, 2008: 3643-3648. https://doi.org/10.1007/s10853-008-2580-7

[14] M. Sona, K.N. Prabhu. Review on microstructure evolution in Sn–Ag–Cu solders and its effect on mechanical integrity of solder joints. *Journal of Materials Science: Materials in Electronics*, 24, 2013: 3149–3169. https://doi.org/10.1007/s10854-013-1240-0

[15] A. Zribi, A. Clark, L. Zavalij, P. Borgesen, E.J. Cotts, The growth of intermetallic compounds at Sn-Ag-Cu solder/Cu and Sn-Ag-Cu solder/Ni interfaces and the associated evolution of the solder microstructure. *Journal of Electronic Materials*, 30, 2001: 1157-1164. https://doi.org/10.1007/s11664-001-0144-6

[16] A.R. Fix, G.A. Lopez, I. Brauer, W. Nüchter, E.J. Mittemeijer, Microstructural development of Sn-Ag-Cu solder joints. *Journal of Electronic Materials*, 34, 2005: 137-142. https://doi.org/10.1007/s11664-005-0224-0

[17] Y.W. Wang, Y.W. Lin, C.R. Kao, Kirkendall voids formation in the reaction between Ni-doped SnAg lead-free solders and different Cu substrates. *Microelectronics Reliability*, 49(3), 2009: 248-252. https://doi.org/10.1016/j.microrel.2008.09.010

[18] A.E. Hammad, Evolution of microstructure, thermal and creep properties of Ni-doped Sn0.5Ag0.7Cu low-Ag solder alloys for electronic applications. *Materials & Design*, 52, 2013: 663-670. https://doi.org/10.1016/j.matdes.2013.05.102

[19] D. Zhou, A.S.M.A. Haseeb, A. Andriyana, Mechanical performance of advanced multicomponent lead-free solder alloy under thermal aging. *Materials Today Communications*, 33, 2022: 104-430. https://doi.org/10.1016/j.mtcomm.2022.104430

[20] K.S. Kim, S.H. Huh, K. Suganuma, Effects of fourth alloying additive on microstructures and tensile properties of Sn-Ag-Cu alloy and joints with Cu. *Microelectronics Reliability*, 43(2), 2003: 259-267. https://doi.org/10.1016/S0026-2714(02)00239-1

[21] A.A. El-Daly, A.E. Hammad, A. Fawzy, D.A. Nasrallh, Microstructure, mechanical properties, and deformation behavior of Sn1.0Ag0.5Cu solder after Ni and Sb additions. *Materials & Design*, 43, 2013: 40-49. https://doi.org/10.1016/j.matdes.2012.06.058

[22] H.-K. Cheng, C.-W. Huang, H. Lee, Y.-L. Wang, T.-F. Liu, C.-M. Chen, Interfacial reactions between Cu and SnAgCu solder doped with minor Ni. *Journal of Alloys and Compounds*, 622, 2015: 529-534. https://doi.org/10.1016/j.jallcom.2014.10.121

[23] G. Zeng, S.D. McDonald, Q. Gu, Y. Terada, K. Uesugi, H. Yasuda, K. Nogita, The influence of Ni and Zn additions on microstructure and phase transformations in Sn0.7Cu/Cu solder joints. *Acta Materialia*, 83, 2015: 357-371. https://doi.org/10.1016/j.actamat.2014.10.003

[24] A.E. Hammad, Enhancing the ductility and mechanical behavior of Sn-1.0Ag-0.5Cu lead-free solder by adding trace amount of elements Ni and Sb. *Microelectronics Reliability*, 87, 2018: 133-141. https://doi.org/10.1016/j.microrel.2018.06.015

[25] A. Hammad, A. El-Taher, Mechanical deformation behaviour of Sn-Ag-Cu solders with minor addition of 0.05 wt.% Ni. *Journal of Electronic Materials*, 43, 2014: 4146-4157. https://doi.org/10.1007/s11664-014-3323-y

[26] F.X. Che, W.H. Zhu, E.S.W. Poh, X.W. Zhang, X.R. Zhang, The study of mechanical properties of SnAgCu lead-free solders with different Ag contents and Ni doping under different strain rates and temperatures. *Journal of Alloys and Compounds*, 507(1), 2010: 215-224. https://doi.org/10.1016/j.jallcom.2010.07.160

[27] A.A. El-Daly, A.M. El-Taher, T.R. Dalloul, Enhanced ductility and mechanical strength of Ni-doped Sn3.0Ag0.5Cu lead-free solders. *Materials & Design*, 55, 2014: 309-318. https://doi.org/10.1016/j.matdes.2013.10.009

[28] K. Nogita, Stabilisation of Cu_6Sn_5 by Ni in Sn-0.7Cu-0.05Ni lead-free solder alloys. *Intermetallics*, 18(1), 2010: 145-149. https://doi.org/10.1016/j.intermet.2009.07.005

[29] K. Nogita, T. Nishimura, Nickel-stabilized hexagonal $(Cu,Ni)_6Sn_5$ in Sn-Cu-Ni lead-free solder alloys. *Scripta Materialia*, 59(2), 2008: 191-194. https://doi.org/10.1016/j.scriptamat.2008.03.002

[30] C. Yang, F. Song, S.W. Ricky Lee, Impact of Ni concentration on the intermetallic compound formation and brittle fracture strength of Sn-Cu-Ni (SCN) lead-free solder joints. *Microelectronics Reliability*, 54(2), 2014: 435-446. https://doi.org/10.1016/j.microrel.2013.10.005

[31] J. Zhang, L. Zhang, X. Huang, Ch. Wu, K. Deng, W.M. Long, Effect of adding Ni nanoparticles on the melting characteristics, mechanical properties and intermetallic compound growth of Sn58Bi solder. *Soldering & Surface Mount Technology*, 37(1), 2025: 60-70 https://doi.org/10.1108/SSMT-09-2024-0053

[32] K. Nogita, C.M. Gourlay, J. Read, T. Nishimura, S. Suenaga, A.K. Dahle, Effects of phosphorus on microstructure and fluidity of Sn-0.7Cu-0.05Ni lead-free solder. *Materials Transactions*, 49(3), 2008: 443-448 https://doi.org/10.2320/matertrans.MBW200713

[33] A.A. El-Daly, A.M. El-Taher, Improved strength of Ni and Zn-doped Sn-2.0Ag-0.5Cu lead-free solder alloys under controlled processing parameters. *Materials & Design*, 47, 2013: 607-614 https://doi.org/10.1016/j.matdes.2012.12.081